

Electronic Supplementary Information to:

**CTAB-Triggered Ag Aggregates for Reproducible SERS Analysis of Urinary
Polycyclic Aromatic Hydrocarbon Metabolites**

Ye Gao,[†] Linfang Li,[†] Xue Zhang,^{†,‡} Xinnan Wang,[†] Wei Ji,^{*,†} Jianzhang Zhao,[‡] and Yukihiro
Ozaki[§]

[†]School of Chemistry, Dalian University of Technology, Dalian 116024, P. R. China

[‡]State Key Laboratory of Fine Chemicals, School of Chemical Engineering, Dalian University of
Technology, Dalian 116024, P. R. China.

[§]School of Science and Technology, Kwansai Gakuin University, 2-1 Gakuen, Sanda, Hyogo 669-
1337, Japan

* Correspondence and requests for materials should be addressed to W. J. (E-mail:

jiwei@dlut.edu.cn).

A. Experimental Section

Chemicals and Reagents. Silver nitrate was purchased from Sigma-Aldrich (St. Louis, Mo, USA). CTAB, 2-hydroxynaphthalene (2-OHNap), 1-hydroxypyrene (1-OH-Pyr), and 9-hydroxyfluorene (9-OHFlu) were obtained from Aladdin Chemistry Co. Ltd. (Shanghai, China). 6-Hydroxychrysene (6-OHChr), 3-hydroxybenzo[a]pyrene (3-OHBaP), chrysene (Chr), and benzo[a]pyrene (BaP) were obtained from J&K Scientific Ltd. (Beijing, China). 1-hydroxypyrene glucuronide (1-OHPyr-Glu) was obtained from Yuanye Bio-Technology Co. Ltd. (Shanghai, China). Other chemicals were acquired from Beijing Chemical Reagent Factory (Beijing, China). Urine samples used for evaluating the method were donated by a nonoccupationally exposed volunteer. Spiked urine samples were obtained by directly diluting 10^{-3} M of 1-OHPyr in urine. All of the reagents were of analytical grade and used without further purification. Ultrapure water ($18.2 \text{ M}\Omega \text{ cm}$) was used for all experiments.

Preparation of Ag NPs. The silver colloid was prepared using a conventional synthetic route.⁴³ Briefly, 200 mL of a 1.0 mM aqueous silver nitrate solution was added to 250 mL three-neck bottles and then heated to $85 \text{ }^\circ\text{C}$ with rapid stirring under reflux. A 4 mL solution of 1% trisodium citrate was added to the solution, after which it was boiled for 45 min.

SERS assay. OH-PAHs with different concentrations were prepared in ethanol. For SERS studies, 100 μL CTAB was mixed with 800 μL Ag NPs and shaken thoroughly for 1 min. And then 100 μL OH-PAHs with different concentrations was added into the mixture and incubated for 20 min. The data acquisition time was usually 10 seconds with two accumulations for each measurement. The error bars represent standard deviations based on five independent measurements. The Raman band of silicon wafer at 520.7 cm^{-1} was used to calibrate the spectrometer. The obtained SERS spectra of OH-PAHs were first processed by carrying baseline correction and smoothing to remove the background and noise in SERS measurements. And then, the SERS spectra were further normalized to the intensity of the signal due to CTAB at 758 cm^{-1} .

Instruments. UV-vis spectra were recorded on a Shimadzu UV-2550 spectrophotometer. Dynamic light scattering (DLS) and zeta-potential were measured using Malvern Zetasizer Nano ZS90. SERS spectra were measured by a portable Raman instrument (SERS-ID, Real-Time Analyzers, Inc., USA) with the excitation wavelength of 785 nm (30 mW). The laser spot size was about 30-50 micrometer in the SERS measurements.

B. Additional Figures.

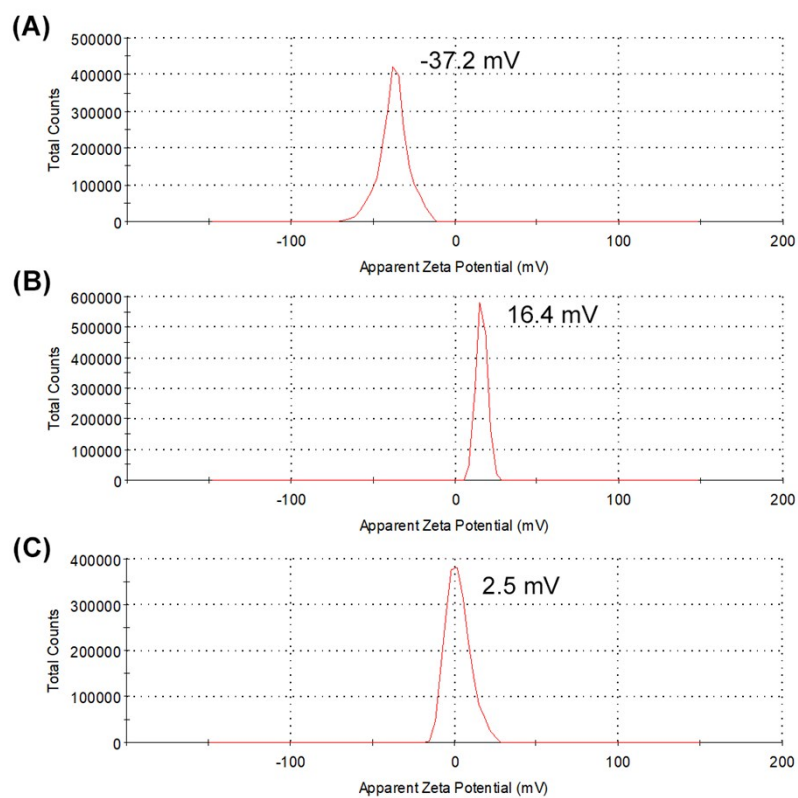


Fig. S1 Zeta potential of Ag nanoparticles in the (A) absence and (B) presence of CTAB. (C) Zeta potential of CTAB-triggered Ag aggregates after addition of 1-OHPyr.

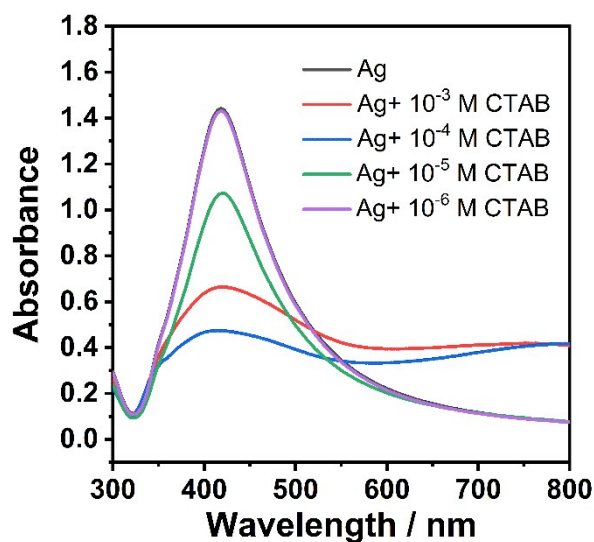


Fig. S2 UV-Vis absorption spectra of Ag NPs with different concentrations of CTAB. The UV-Vis absorption spectrum of the Ag NPs shows a maximum absorption at 420 nm. The addition of CTAB results in a marked intensity decrease of the original absorption peak as well as the appearance of new broad band at around 800 nm, corresponding to the absorption characteristic of the closely spaced Ag NPs. This result indicates the agglomerate of Ag NPs, and the aggregation degree gradually increased with an increase in the amount of CTAB. However, the degree of aggregation of Ag NPs decreases when the concentration of CTAB is higher than 10^{-3} M. This may be due to the formation of CTAB bilayer on Ag NPs surface, which impeded the aggregation of Ag NPs.

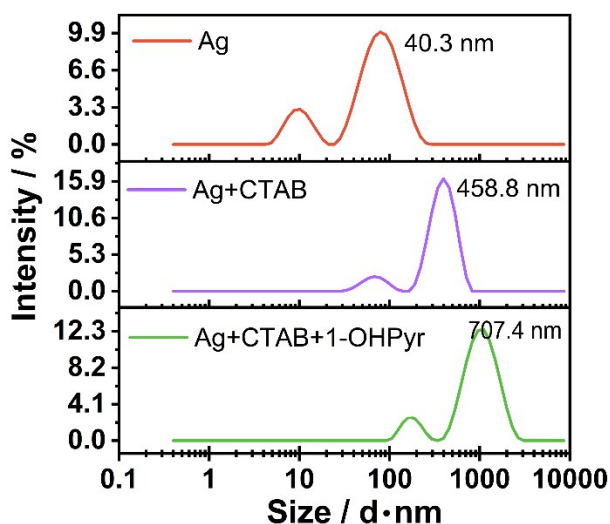


Fig. S3 Dynamic light scattering analysis of Ag NPs without and with CTAB (10^{-4} M), and CTAB-triggered Ag aggregates in the presence of 1-OHPyr (10^{-5} M). The average hydrodynamic diameter of Ag NPs is 40.3 nm, which is identical to that observed previously for citrate-reduced Ag NPs. After addition of CTAB, the average hydrodynamic diameter of Ag NPs increases to 458.8 nm, indicating the formation of Ag aggregates.

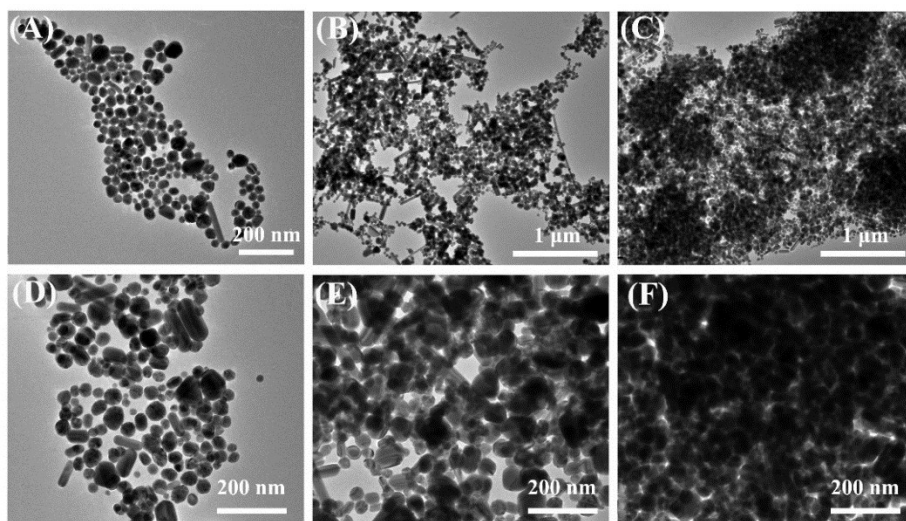


Fig. S4 TEM of (A) and (D) Ag nanoparticles, (B) and (E) CTAB-triggered Ag aggregates, and (C) and (F) CTAB-triggered Ag aggregates after addition of 1-OHPyr. It can be seen that the Ag colloids are near dispersed. However, the addition of CTAB leads to the formation of Ag aggregates and the degree of aggregation increases after the introduction of 1-OHPyr.

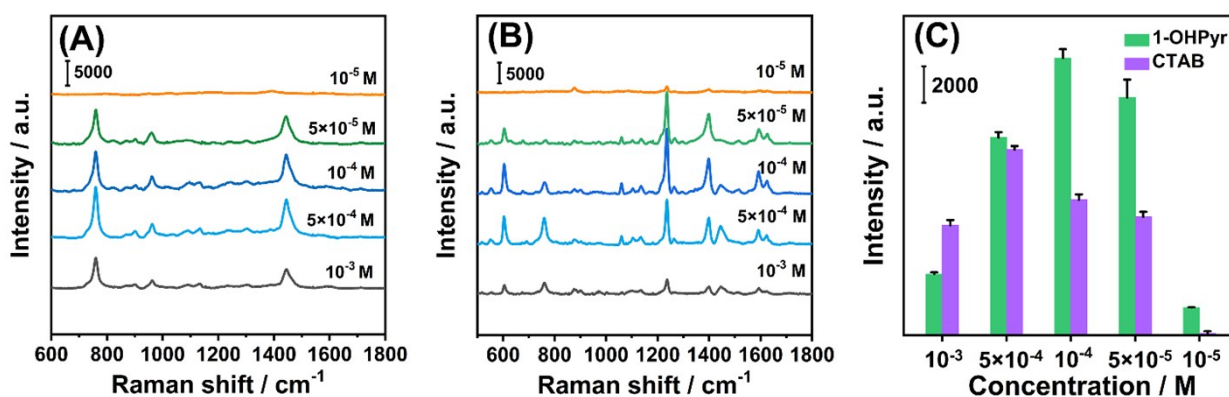


Fig. S5 (A) SERS spectra of CTAB with different concentrations. (B) The CTAB concentration-dependent SERS spectra of 1-OHPyr in CTAB-triggered Ag aggregates. (C) The CTAB concentration-dependent SERS intensities of the CTAB band at 759 cm^{-1} and the 1-OHPyr (10^{-5} M) band at 1236 cm^{-1} . When the amount of CTAB was insufficient, no SERS signal of 1-OHPyr was observed just as in the case of bare Ag NPs. The SERS intensity increased on increasing the concentration of CTAB and was maximized at 10^{-4} M CTAB, while the SERS intensity obviously decreased as the concentration was higher than $5 \times 10^{-4} \text{ M}$. This could be attributed to the fact that the CTAB with higher concentrations could form an intact CTAB bilayer that repels the analytes adsorbed on the Ag surface. Furthermore, excessive CTAB will also form micelles, which could also capture the 1-OHPyr, thereby resulting in the decrease in SERS intensity.

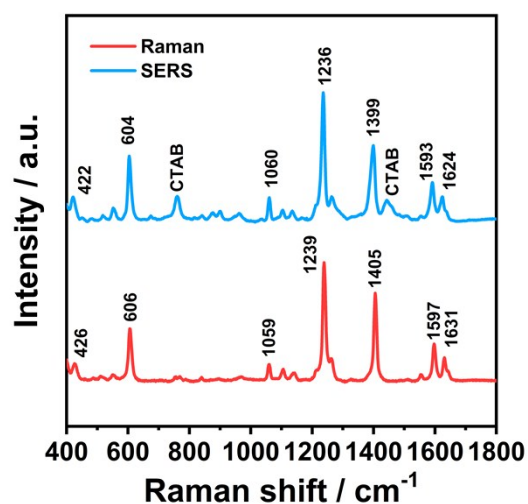


Fig. S6 Typical Raman and SERS spectra of 1-OHPyr.

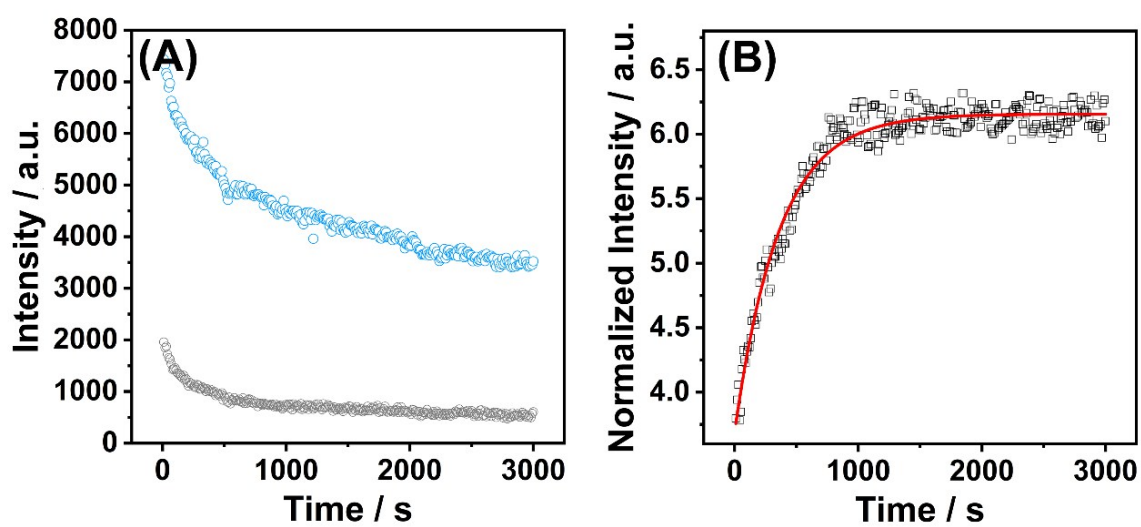


Fig. S7 (A) The time-dependent SERS intensities of 1-OHPyr at 1236 cm^{-1} (blue circle) and CTAB at 758 cm^{-1} (black circle) after addition of 1-OHPyr. (B) The SERS intensity changes of 1-OHPyr as a function of incubation time with CTAB-triggered Ag aggregates.

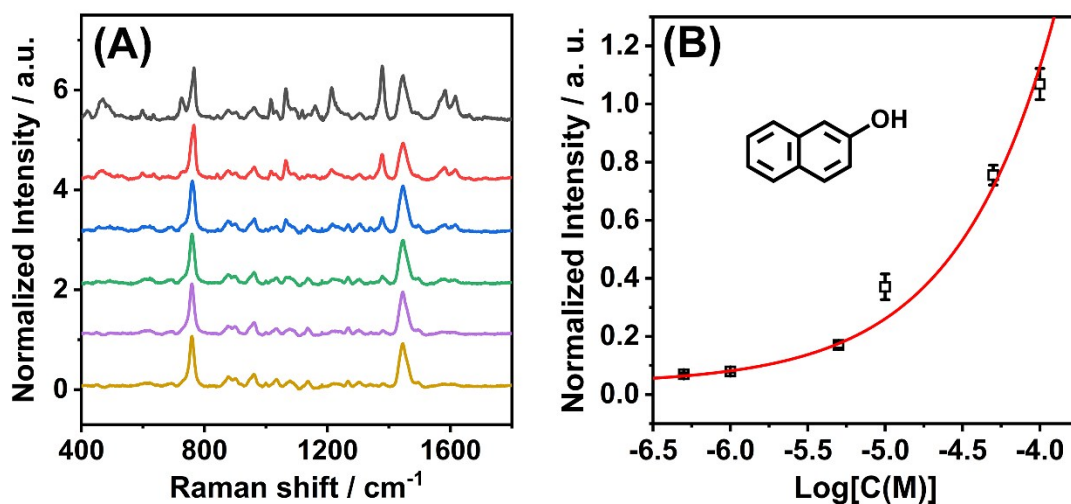


Fig. S8 (A) SERS spectra of 2-OHNap with different concentrations, the concentrations from top to bottom are 10^{-4} , 5×10^{-5} , 10^{-5} , 5×10^{-6} , 10^{-6} , and 5×10^{-7} M. (B) The normalized Raman intensity at 1378 cm^{-1} versus logarithmic 2-OHNap concentration in the mixture.

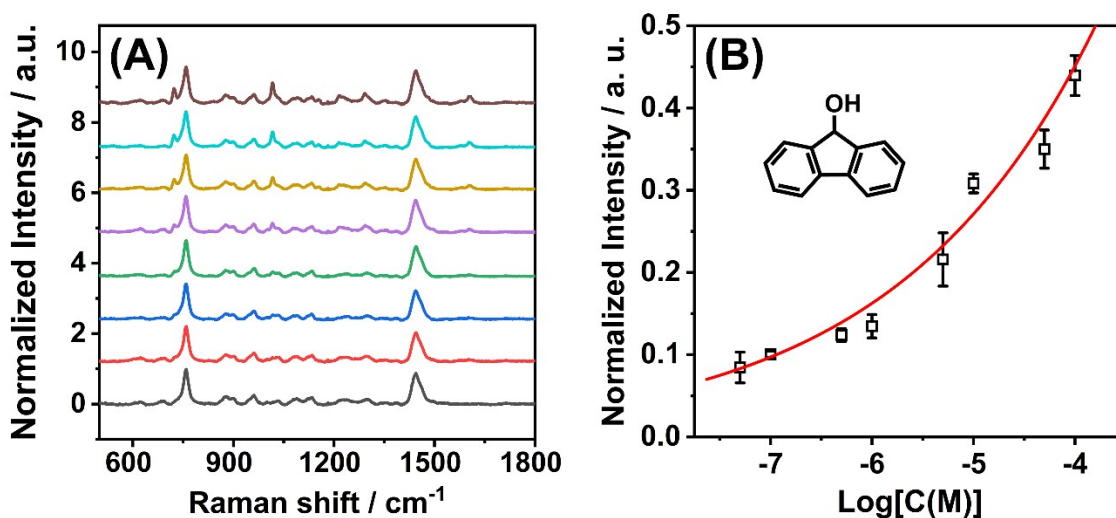


Fig. S9 (A) SERS spectra of 9-OHFlu with different concentrations, the concentrations from top to bottom are 10^{-4} , 5×10^{-5} , 10^{-5} , 5×10^{-6} , 10^{-6} , 5×10^{-7} , 10^{-7} , 5×10^{-8} M. (B) The normalized Raman intensity at 724 cm^{-1} versus logarithmic 9-OHFlu concentration in the mixture.

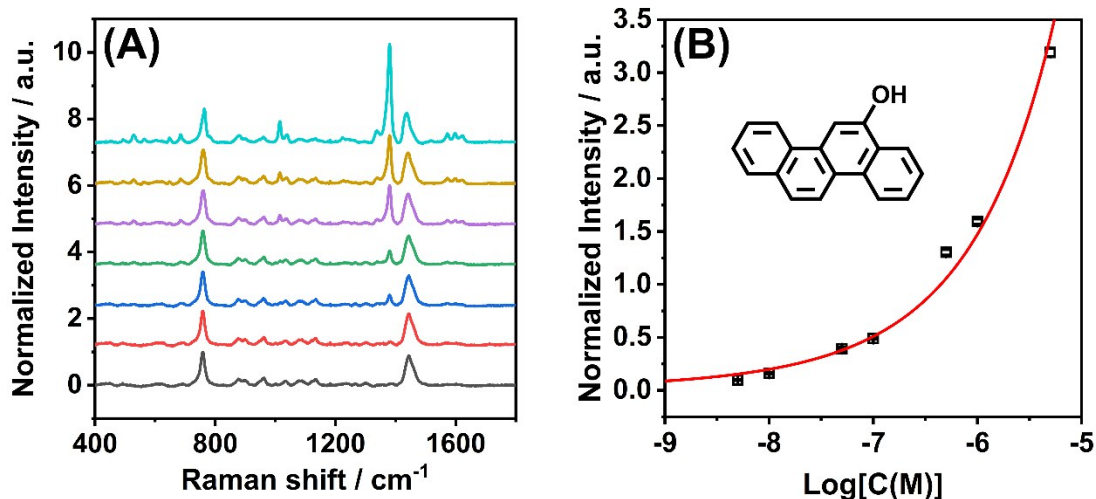


Fig. S10 (A) SERS spectra of 6-OHChr with different concentrations, the concentrations from top to bottom are 5×10^{-6} , 10^{-6} , 5×10^{-7} , 10^{-7} , 5×10^{-8} , 10^{-8} , 5×10^{-9} M. (B) The normalized Raman intensity at 1380 cm^{-1} versus logarithmic 6-OHChr concentration in the mixture.

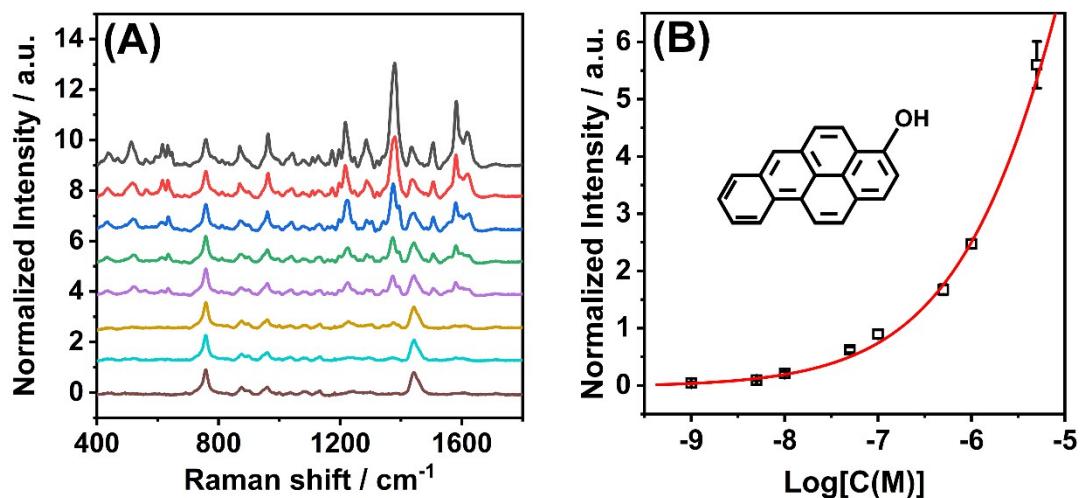


Fig. S11. (A) SERS spectra of 3-OHBaP with different concentrations, the concentrations from top to bottom are 5×10^{-6} , 10^{-6} , 5×10^{-7} , 10^{-7} , 5×10^{-8} , 10^{-8} , 5×10^{-9} , and 10^{-9} M. (B) The normalized Raman intensity at 1379 cm^{-1} versus logarithmic 3-OHBaP concentration in the mixture.

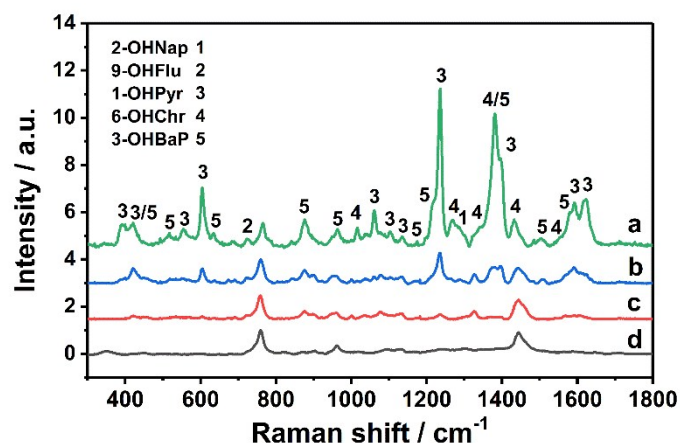


Fig. S12 SERS spectra obtained from a mixture of five kinds of OH-PAHs. a) The concentrations are 1×10^{-4} M for 2-OHNap and 9-OHFlu, 1×10^{-6} M for 1-OHPyr, 6-OHChr, and 3-OHBaP (defined as mixture a), b) ten-fold dilution of mixture a, c) one hundred-fold dilution of mixture a, and d) the concentration of each OH-PAHs is 0 M.

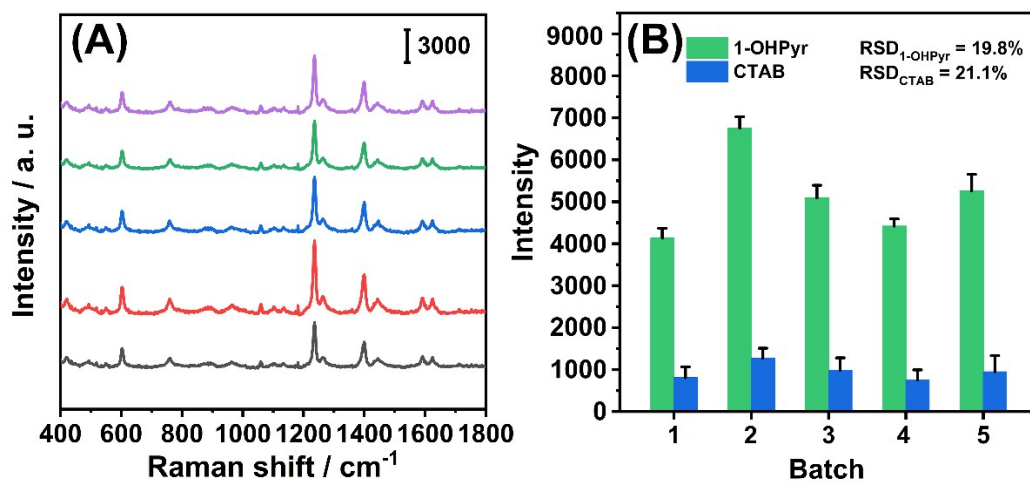


Fig. S13 (A) The SERS spectra of 1-OHPyr by using five batches Ag colloid. (B) The SERS intensities of CTAB at 758 cm^{-1} and urinary 1-OHPyr at 1236 cm^{-1} by using different batches of Ag NPs. It can be seen that the relative standard deviation of both 1-OHPyr signal (1236 cm^{-1}) and CTAB signal (758 cm^{-1}) is calculated to be $\approx 20\%$. However, a better data reproducibility of less 4.6% than relative standard deviation was achieved between batches after correction using the CTAB as the internal standard (Fig. 4B). Obviously, the good reproducibility will improve the accuracy of the quantitative analysis for the OH-PHAs.

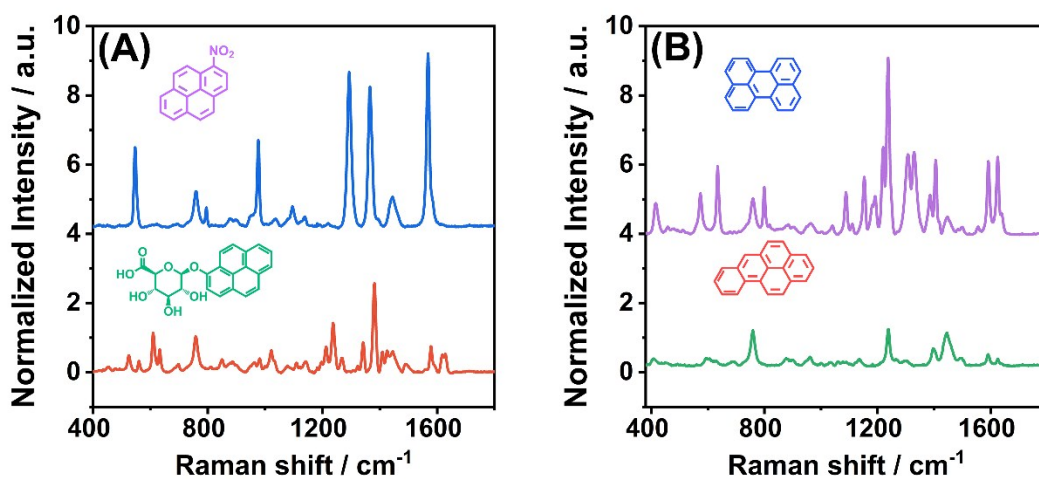


Fig. S14 SERS spectra of perylene, benzo[a]pyrene, 1-nitropyrene, and 1-OHPyr-Glu, each at a concentration of 10^{-5} M. All the intensities of the bands are normalized to the intensity of the signal due to CTAB at 758 cm^{-1} .

Table S1 The assignments of main Raman and SERS peaks for 1-OHPyr.

Raman/ cm^{-1}	SERS/ cm^{-1}	Assignment
1631	1624	CC stretching
1597	1593	CC stretching
1405	1399	CC stretching/ring stretching
1239	1236	CC stretching/CH in-plane bending
1059	1060	CH in-plane bending
606	604	Skeletal stretching
426	422	Skeletal stretching
394	389	Skeletal stretching